Short Article

Cell Metabolism

Palmitic Acid Hydroxystearic Acids Activate GPR40, Which Is Involved in Their Beneficial Effects on Glucose Homeostasis

Graphical Abstract

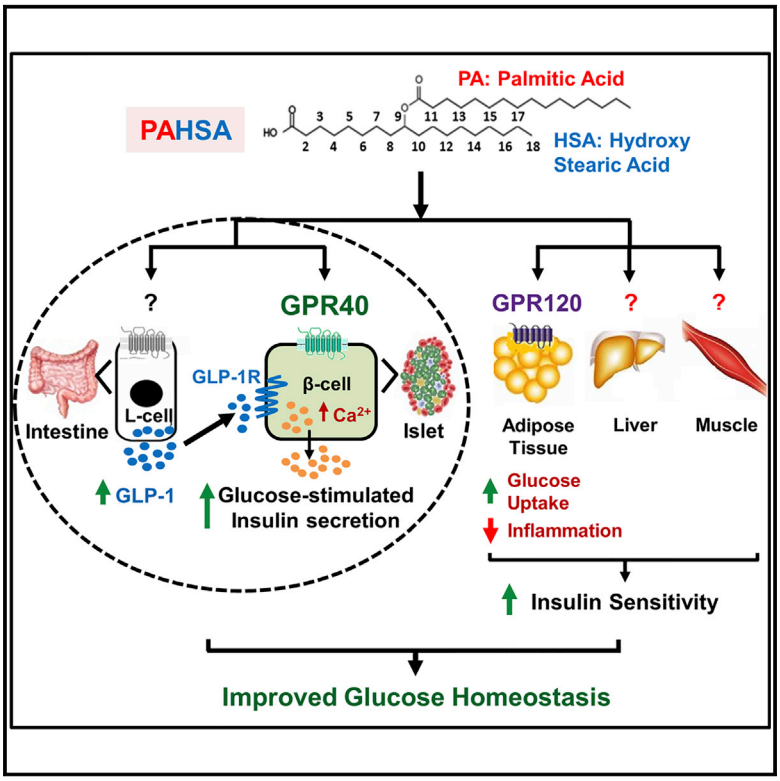

Highlights

- Chronic PAHSA treatment improves insulin sensitivity in chow- and HFD-fed mice
- PAHSAs activate GPR40, which mediates their augmentation of insulin secretion
- GPR40 plays a role in the beneficial effects of PAHSAs on glucose homeostasis
- GLP-1 receptor indirectly mediates PAHSA effects on glucose tolerance

Authors

Ismail Syed, Jennifer Lee, Pedro M. Moraes-Vieira, ..., Odile D. Peroni, Alan Saghatelian, Barbara B. Kahn

Correspondence

bkahn@bidmc.harvard.edu

In Brief

PAHSA levels are reduced in serum and subcutaneous WAT of insulin-resistant people and HFD-fed mice. Restoring PAHSA levels has high therapeutic potential to treat patients with type 2 diabetes. Syed, Lee et al. show that chronic PAHSA treatment improves glucose homeostasis in chow- and HFD-fed mice, and identify GPR40 as a novel PAHSA target.

Syed et al., 2018, Cell Metabolism *27*, 419–427
February 6, 2018
https://doi.org/10.1016/j.cmet.2018.01.001

CellPress

Cell Metabolism
Short Article

Palmitic Acid Hydroxystearic Acids Activate GPR40, Which Is Involved in Their Beneficial Effects on Glucose Homeostasis

Ismail Syed,[1,6] Jennifer Lee,[1,6] Pedro M. Moraes-Vieira,[1,5] Cynthia J. Donaldson,[2] Alexandra Sontheimer,[1] Pratik Aryal,[1] Kerry Wellenstein,[1] Matthew J. Kolar,[2] Andrew T. Nelson,[3] Dionicio Siegel,[3] Jacek Mokrosinski,[4] I. Sadaf Farooqi,[4] Juan Juan Zhao,[1] Mark M. Yore,[1] Odile D. Peroni,[1] Alan Saghatelian,[2] and Barbara B. Kahn[1,7,*]

[1]Division of Endocrinology, Diabetes, and Metabolism, Department of Medicine, Beth Israel Deaconess Medical Center and Harvard Medical School, Center for Life Sciences, Room 747, 330 Brookline Avenue, Boston, MA 02215, USA

[2]Clayton Foundation Laboratories for Peptide Biology, Helmsley Center for Genomic Medicine, Salk Institute for Biological Studies, 10010 North Torrey Pines Road, La Jolla, CA 92037, USA

[3]Skaggs School of Pharmacy and Pharmaceutical Sciences, University of California, San Diego, 9500 Gilman Drive, La Jolla, CA 92093, USA

[4]University of Cambridge Metabolic Research Laboratories and NIHR Cambridge Biomedical Research Centre, Wellcome Trust-MRC Institute of Metabolic Science, Cambridge CB2 0QQ, UK

[5]Present address: Department of Genetics, Evolution, Microbiology, and Immunology, Institute of Biology, University of Campinas, Campinas-SP 13083-970, Brazil

[6]These authors contributed equally

[7]Lead Contact

*Correspondence: bkahn@bidmc.harvard.edu

https://doi.org/10.1016/j.cmet.2018.01.001

SUMMARY

Palmitic acid hydroxystearic acids (PAHSAs) are endogenous lipids with anti-diabetic and anti-inflammatory effects. PAHSA levels are reduced in serum and adipose tissue of insulin-resistant people and high-fat diet (HFD)-fed mice. Here, we investigated whether chronic PAHSA treatment enhances insulin sensitivity and which receptors mediate PAHSA effects. Chronic PAHSA administration in chow- and HFD-fed mice raises serum and tissue PAHSA levels ~1.4- to 3-fold. This improves insulin sensitivity and glucose tolerance without altering body weight. PAHSA administration in chow-fed, but not HFD-fed, mice augments insulin and glucagon-like peptide (GLP-1) secretion. PAHSAs are selective agonists for GPR40, increasing Ca^{+2} flux, but not intracellular cyclic AMP. Blocking GPR40 reverses improvements in glucose tolerance and insulin sensitivity in PAHSA-treated chow- and HFD-fed mice and directly inhibits PAHSA augmentation of glucose-stimulated insulin secretion in human islets. In contrast, GLP-1 receptor blockade in PAHSA-treated chow-fed mice reduces PAHSA effects on glucose tolerance, but not on insulin sensitivity. Thus, PAHSAs activate GPR40, which is involved in their beneficial metabolic effects.

INTRODUCTION

Type 2 diabetes (T2D) is a global epidemic (International Diabetes Federation, 2013) characterized by hyperglycemia due to impaired islet function and insulin resistance in peripheral tissues. Despite advances in understanding the molecular mechanisms contributing to T2D and the development of new treatment modalities, the medical management of T2D remains inadequate (Aroda et al., 2012). At present, many available treatment strategies including analogs of the incretin, glucagon-like peptide 1 (GLP-1), and dipeptidylpeptidase-4 inhibitors work primarily by increasing insulin secretion. Other effective agents promote glucose excretion (Campbell and Drucker, 2013; Meier, 2012). However, there is still a need for effective and safe agents that enhance insulin sensitivity to improve glucose control and prevent diabetic complications.

We discovered a novel class of endogenous lipids, branched fatty acid esters of hydroxy fatty acids (FAHFAs), with beneficial metabolic and anti-inflammatory effects (Yore et al., 2014). More than 16 FAHFA family members have been identified (Yore et al., 2014; Ma et al., 2015). Levels of one of the FAHFA family members, palmitic acid hydroxystearic acid (PAHSA), are markedly lower in serum and adipose tissue (AT) of insulin-resistant humans. PAHSA levels correlate strongly with insulin sensitivity as measured by euglycemic clamps in humans (Yore et al., 2014). Acute oral treatment with 5- or 9-PAHSA isomer in chow-fed and high-fat diet (HFD)-fed mice improves glucose tolerance and augments insulin and GLP-1 secretion *in vivo*. *In vitro*, PAHSAs directly enhance GLP-1 secretion from enteroendocrine cells and glucose-stimulated insulin secretion (GSIS) from human islets (Yore et al., 2014). Furthermore, PAHSAs have anti-inflammatory effects including decreasing AT inflammation in HFD mice and attenuating lipopolysaccharide-induced dendritic cell activation and cytokine production. Although we reported that a single dose of PAHSAs acutely improves glucose tolerance, whether PAHSAs have effects on insulin sensitivity has not been investigated. Therefore, the first aim of this study was to determine whether PAHSA treatment enhances insulin sensitivity *in vivo*, and the second aim was to

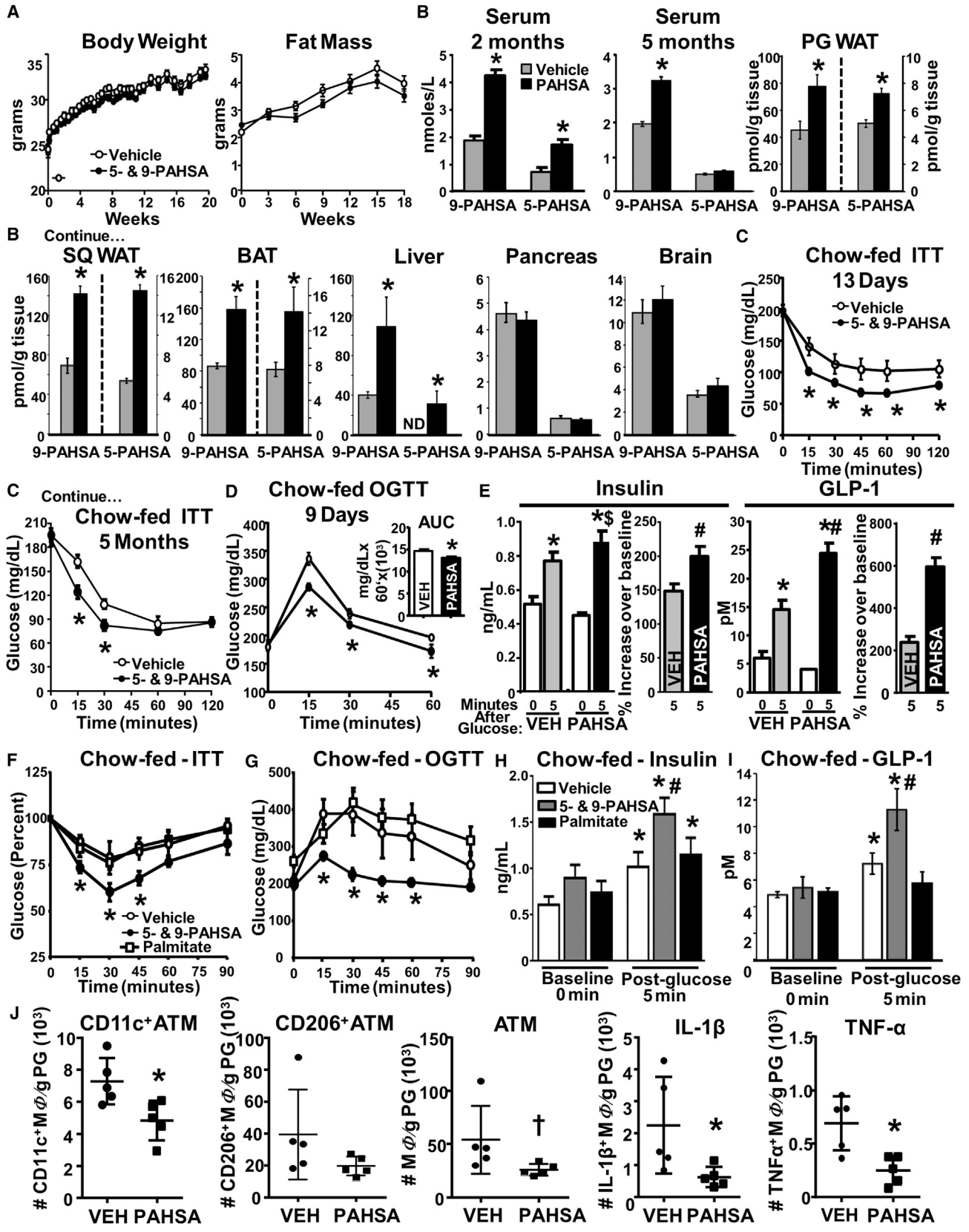

(legend on next page)

determine whether the beneficial effects of PAHSAs are sustained with chronic treatment.

The receptors responsible for PAHSA effects on insulin secretion and insulin action *in vivo* have not been identified. The G protein-coupled receptor (GPCR) GPR120 mediates PAHSA effects to enhance insulin-stimulated glucose transport in adipocytes (Yore et al., 2014), but PAHSAs are likely to activate other GPCRs because of their diverse actions in multiple tissues. Major pharmaceutical companies have had high-priority programs to screen for GPR120 and GPR40 activators to treat T2D. Molecules that activate both of these GPCRs with naturally evolved relative affinities may be more effective for T2D treatment than agonists for single receptors.

Recent research has focused on identifying key agonists and receptors mediating nutrient-induced GLP-1 and insulin secretion. The long-chain fatty acid receptor GPR40 is the most abundant GPCR expressed in islet β cells and is also expressed on intestinal L-cells, where it contributes to GLP-1 release along with GPR120 (Itoh et al., 2003; Edfalk et al., 2008). GPR40 activation augments GSIS and improves glycemia in rodent T2D models (Itoh et al., 2003; Steneberg et al., 2005), and the GPR40 agonist TAK-875 lowers fasting and postprandial blood glucose and HbA1c levels in humans (Leifke et al., 2012; Burant et al., 2012). Because PAHSAs acutely augment GSIS directly from human islets (Yore et al., 2014), the third aim of this study was to determine whether PAHSAs activate GPR40 and whether this contributes to their beneficial effects *in vivo*. Here we show that PAHSAs directly activate GPR40, which is important for PAHSA effects on glucose homeostasis in both chow and HFD mice.

Since PAHSAs augment GLP-1 secretion in insulin-resistant mice (Yore et al., 2014), we also investigated the role of the GLP-1 receptor (GLP-1R) in mediating PAHSA effects on glucose metabolism. GLP-1 potentiates insulin secretion and suppresses glucagon release (Holst, 2007), but its beneficial actions are not limited to the endocrine pancreas (Ayala et al., 2009; Christensen et al., 2015; Villanueva-Peñacarrillo et al., 2011). Here we show that the GLP-1R contributes to the beneficial PAHSA effects on insulin secretion and glucose tolerance, but not on insulin sensitivity, in chow mice. In addition, PAHSA-stimulated augmentation of GSIS in chow mice is directly mediated by GPR40, but their effects on GLP-1 secretion do not involve GPR40. Thus, PAHSAs improve glucose tolerance and insulin sensitivity in chow mice and these effects are sustained for 5 months. In HFD mice, glucose tolerance and insulin sensitivity are also improved by PAHSA treatment, but the effects are more modest. Furthermore, this study shows that PAHSAs directly activate GPR40, which contributes to their beneficial metabolic effects in mice on both chow and HFD.

RESULTS AND DISCUSSION

Chronic PAHSA Treatment Improves Insulin Sensitivity and Glucose Tolerance and Reduces Adipose Tissue Inflammation in Chow-Fed Mice without Altering Food Intake or Adiposity

5- and 9-PAHSA treatment for up to 18 weeks in chow mice had no effect on body weight, fat mass (Figure 1A), food intake, lean mass, serum triglycerides, or free fatty acid (FFA) levels (Figures S1A and S1B). Serum 5- and 9-PAHSA levels increased 2-fold with 2 months of treatment compared with vehicle mice (Figure 1B). After 5 months of treatment, only 9-PAHSA levels were elevated in serum (Figure 1B). However, 5- and 9-PAHSA levels were increased 1.5- to 3-fold in perigonadal (PG) and subcutaneous (SC) white AT (WAT) and brown AT. In liver, 9-PAHSA levels were elevated 2.5-fold in PAHSA-treated mice, and 5-PAHSA was detected even though this isomer was not found in liver of vehicle-treated mice as expected (Yore et al., 2014) (Figure 1B). 5- and 9-PAHSA levels were not increased in the pancreas or brain with chronic PAHSA treatment (Figure 1B).

5- and 9-PAHSA treatment improved insulin sensitivity as early as 13 days of treatment, and these effects were sustained for at least 5 months (Figure 1C). Glucose tolerance (Figure 1D) was also improved, similar to the effects reported with a single dose (Yore et al., 2014). Loss of first-phase insulin response to glucose is one of the major and early impairments of β cell function in T2D (Luzi and DeFronzo, 1989). Restoration of this response is associated with improvements in postprandial glucose excursions (Bruce et al., 1987). Chronic 5- and 9-PAHSA treatment enhances insulin secretion in response to glucose by 40% over vehicle-treated mice (Figure 1E, left panel). In PAHSA-treated mice, GLP-1 levels tended to be reduced at baseline but the stimulation in response to glucose was enhanced 225% over vehicle mice (Figure 1E, right panel). Thus, not only does an acute oral dose of PAHSAs improve first-phase insulin and GLP-1 responses to glucose, but this effect is maintained over 5 months without tachyphylaxis or β cell exhaustion. To confirm that the beneficial effects of PAHSAs on metabolic parameters are distinct from effects of ordinary FFAs, we performed similar studies with palmitate since PAHSAs are made up of palmitate and hydroxystearic acid.

Figure 1. Chronic PAHSA Treatment Improves Insulin Sensitivity and Glucose Tolerance, and Reduces Adipose Tissue Inflammation without Altering Food Intake or Adiposity

(A) Body weight and fat mass of C57bl6 male chow mice treated with vehicle or 5- and 9-PAHSAs (2 mg/kg body weight/day of each) via minipumps. n = 16/group.

(B) 5- and 9-PAHSA levels in sera at 2 and 5 months, and tissues at 5 months of 5- and 9-PAHSA treatment. n = 5–6/group.

(C and D) Insulin tolerance tests (ITTs) (C) and oral glucose tolerance tests (OGTTs) (D) in vehicle- and PAHSA-treated mice. n = 8–11/group.

For (A)–(D), *$p < 0.05$ versus vehicle.

(E) Serum insulin and GLP-1 levels 5 min post-glucose challenge in vehicle- and PAHSA-treated mice. n = 14–16/group. *$p < 0.05$ versus baseline within same treatment, $^{\#}p < 0.05$ versus vehicle at same time point, $^{\$}p = 0.08$ versus vehicle at same time point.

(F–I) ITT (F), OGTT (G), and serum insulin and GLP-1 (H and I) levels 5 min post-glucose challenge in vehicle-, palmitate-, and PAHSA-treated outbred mice. n = 7–9/group. *$p < 0.05$ versus baseline within same treatment, $^{\#}p < 0.05$ versus vehicle at same time point.

(J) Number of AT $CD11c^+$, $CD206^+$, total number of AT macrophages, and macrophages expressing IL-1β and TNF-α from PG WAT. n = 4–5/group. *$p < 0.05$ versus vehicle, $^{\dagger}p < 0.08$ versus vehicle.

Statistical significance was evaluated by unpaired two-tailed Student's t test or two-way ANOVA with Tukey post hoc tests. Data are means ± SEM.

Palmitate treatment at the same dose used for PAHSAs did not have favorable effects on glucose tolerance, insulin tolerance, or glucose-stimulated insulin or GLP-1 secretion (Figures 1F–1I). In addition, unlike palmitate, which depletes islet insulin content with chronic exposure, PAHSA treatment of human islets for 72 hr results in sustained potentiation of GSIS and no loss of insulin content (data not shown).

In addition, at the same concentration as PAHSAs (20 μM), palmitate did not augment GSIS in pancreatic MIN6 β cells (Figure S1C). This was not because of lower palmitate uptake into cells, since lipid uptake measured as the ratio of labeled PAHSA or $^{13}C_{16}$-palmitate within the cell (high-density microsomes, low-density microsomes, and cytosol fractions) compared with plasma membranes was higher for palmitate than for PAHSAs (data not shown).

We next investigated whether chronic PAHSA treatment reduces AT inflammation. PAHSA treatment reduced the total number of AT CD11c$^+$ (pro-inflammatory) macrophages with no effect on AT CD206$^+$ (anti-inflammatory) macrophages (Figures 1J and S1D). The total number of AT macrophages tended to be reduced with PAHSA treatment (Figure 1J) with no change in monocytes or neutrophils (Figures S1E and S1F). Moreover, PAHSA treatment reduced the number of pro-inflammatory interleukin-1β (IL-1β) and tumor necrosis factor α (TNF-α) AT macrophages (Figure 1J). Together, these data indicate that chronic PAHSA treatment reduces AT inflammation, which could contribute to enhanced glucose homeostasis in chow mice.

PAHSAs Activate GPR40 and This Plays a Role in Their Effects on Insulin Secretion

Since FFAs can induce insulin secretion through GPR40, we studied the role of GPR40 in mediating PAHSA effects. 9-PAHSA potentiated GSIS in isolated human islets, and this effect was completely reversed with the GPR40 antagonist, GW1100 (Figure 2A). Similarly, GPR40 knockdown in MIN6 cells completely reversed 9-PAHSA-potentiated GSIS without altering insulin secretion at low glucose (Figures 2B and S2A). Thus, both genetic and pharmacologic approaches indicate that PAHSAs augment GSIS by activating GPR40.

To determine whether PAHSAs directly activate GPR40, we transfected HEK293 cells with mouse GPR40 and SRE-luc. 9-PAHSA dose-dependently activates GPR40 (Figure 2C). 5-PAHSA also activates GPR40 (Figure S2B). PAHSAs also directly activate human GPR40 (data not shown). 9-PAHSA-induced GPR40 activation was attenuated by GW1100 in a dose-dependent manner (Figure 2D). We next determined whether PAHSAs are full or selective GPR40 agonists. 9-PAHSA increased Ca^{+2} flux similar to the positive control linoleic acid, and GW1100 attenuated this effect (Figure 2E). However, 9-PAHSA had no effect on intracellular cyclic AMP (cAMP) levels (Figure 2F). Thus, PAHSAs are selective, not full, agonists for GPR40. We also tested whether GPR40 directly mediates PAHSA effects on GLP-1 secretion in STC-1 enteroendocrine cells. Both 5- and 9-PAHSAs augmented GLP-1 secretion in STC-1 cells by 1.5- to 2-fold, but GPR40 antagonism did not reduce this effect (Figure S2C). This suggests that PAHSA augmentation of GLP-1 secretion in enteroendocrine cells is independent of GPR40.

Inhibition of GPR40 Reverses the Beneficial Effects of 5- and 9-PAHSA on Both Glucose Tolerance and Insulin Sensitivity

To determine whether PAHSA effects on GSIS are mediated by GPR40 *in vivo*, we injected vehicle- and 5- and 9-PAHSA-treated chow mice with DC260126, a GPR40 antagonist. DC260126 attenuated the beneficial effects of PAHSAs on insulin sensitivity and glucose tolerance (Figures 2G and 2H compared with Figures 1C and 1D), but had no effect on vehicle-treated mice (Figures S2D–S2F). There was no effect of GPR40 inhibition on glycemia at baseline or 5 min after glucose gavage (Figures 2I and S2G). However, GPR40 inhibition lowered baseline insulinemia (30 min after DC260126) and completely blocked GSIS in PAHSA-treated mice (Figure 2I). In vehicle-treated mice, DC260126 also tended to impair GSIS (Figure S2G). The fact that DC260126 blocked the glucose effect on insulin secretion as well as the PAHSA effects may be because DC260126 inhibits an increase in intracellular Ca^{+2} (Hu et al., 2009), possibly by modifying ligand-independent GPR40 activity (Milligan et al., 2017). In PAHSA- and vehicle-treated mice, GPR40 inhibition did not affect glucose-stimulated GLP-1 secretion (Figures 2I and S2G). Thus, PAHSAs stimulate insulin secretion through GPR40 but their effects on GLP-1 secretion do not involve GPR40. The conclusion that DC260126 inhibition of PAHSA-mediated potentiation of insulin secretion *in vivo* (Figure 2I, middle panel) involves GPR40 is supported by the *in vitro* data using another GPR40 antagonist, GW1100 (Figure 2D), and genetic knockdown of GPR40 in β cells (Figure 2B). In terms of the specificity of DC260126, it had no effect on PAHSA activation of another lipid-responsive GPCR, GPR43 (data not shown). Specificity was also tested by Hu et al. (2009) using a calcium mobilization assay with GPR40 or melanin concentrating hormone receptor 2 (MCHR2), another GPCR of the same subtype $G_{\alpha q/11}$. DC260126 dose-dependently inhibited FFA-induced GPR40 activation, but had no effect on MCHR2 activation by its ligand, melanin concentrating hormone (Hu et al., 2009). Extensive testing for the specificity of DC260126 has not been done, but the lack of effect in vehicle-treated mice (Figures S2E and S2F) reduces the possibility of off-target effects.

We also determined whether the effects of chronic PAHSA treatment *in vivo* are sustained in islets *ex vivo*. There was no augmentation of GSIS in islets from PAHSA-treated mice *ex vivo* compared with islets from vehicle mice (Figure S2H). This suggests that the continuous presence of PAHSAs is required to trigger the GPR40 activity.

GLP-1R Blockade Reverses the Beneficial Effects of Chronic PAHSA Treatment on Glucose Tolerance, but Not Insulin Sensitivity

To determine whether PAHSA-induced improvements in glucose tolerance and insulin sensitivity are mediated through enhanced GLP-1 secretion, we injected vehicle- and 5- and 9-PAHSA-treated chow mice with the GLP-1R antagonist Exendin(9–39) (Ex(9–39)) (Figure 3A). Ex(9–39) completely reversed PAHSA-induced improvements in glucose tolerance (Figures 3B and S3A), but not insulin sensitivity (Figure 3C). In PAHSA-treated mice, GLP-1R blockade increased glycemia at baseline (30 min after Ex(9–39)) (Figures 3B–3D) and at 5 min after glucose administration (Figure 3D). In addition, Ex(9–39)

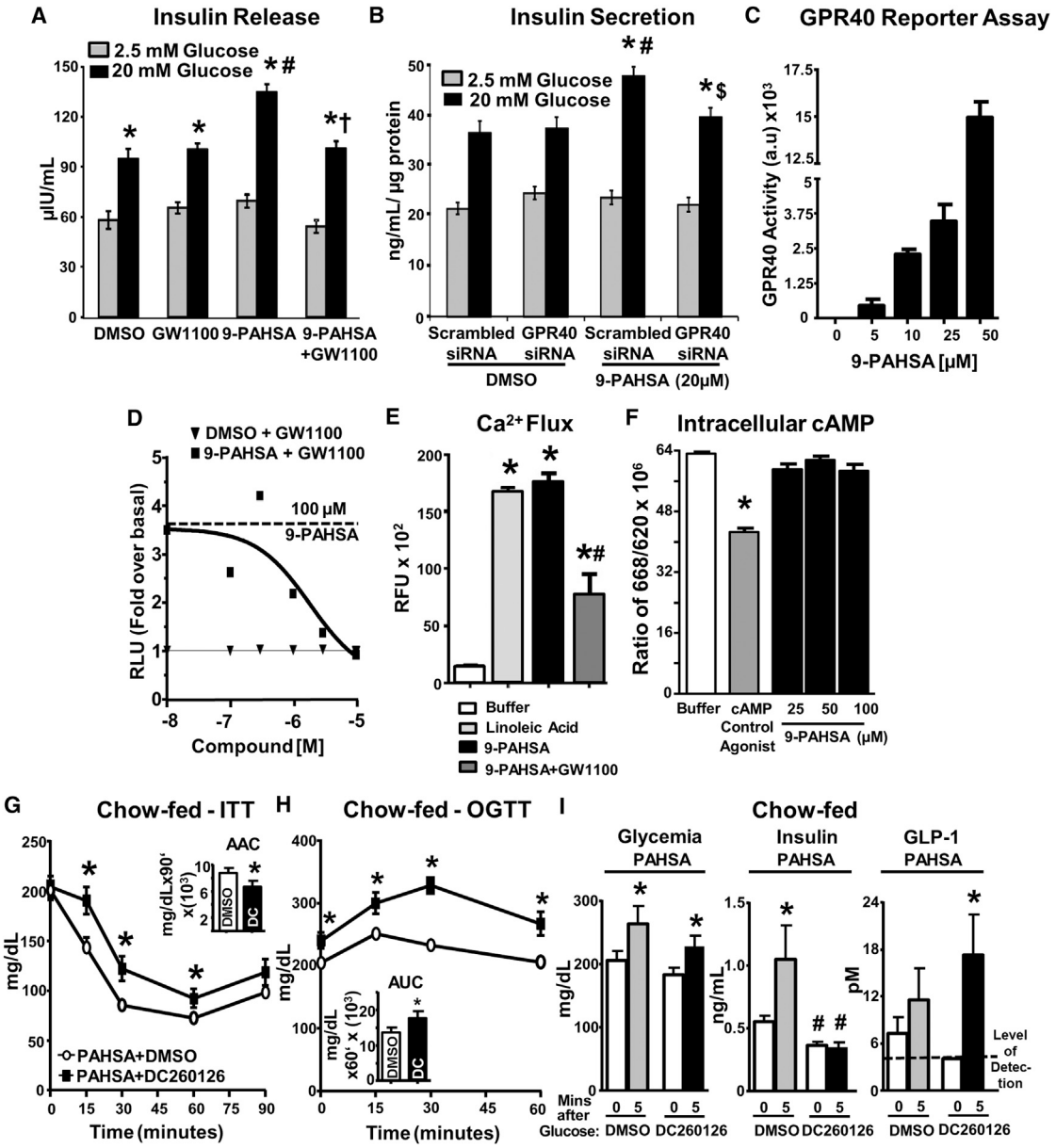

Figure 2. PAHSAs Directly Activate GPR40, and GPR40 Antagonism Reverses PAHSA-Mediated Improvements in Glucose Tolerance, Insulin Sensitivity, and Insulin Secretion

(A) Human islets treated with DMSO, 9-PAHSA (20 µM), GW1100 (10 µM), or 9-PAHSA + GW1100 for 45 min during glucose stimulation. n = 75 islets/condition. *$p < 0.05$ versus respective 2.5 mM glucose, $^{\#}p < 0.05$ versus DMSO 20 mM glucose, $^{\dagger}p < 0.05$ versus 9-PAHSA 20 mM glucose.

(B) MIN6 cells transfected with scrambled or GPR40 small interfering RNA (siRNA), and treated with DMSO or 9-PAHSA (20 µM) for 45 min during glucose stimulation. n = 10 wells/condition. *$p < 0.05$ versus respective 2.5 mM glucose, $^{\#}p < 0.05$ versus DMSO 20 mM glucose scrambled siRNA, $^{\$}p < 0.05$ versus 9-PAHSA 20 mM glucose scrambled siRNA.

(C) Reporter assay in HEK293 cells transfected with mouse GPR40 and SRE-luc treated with 9-PAHSA. n = 3 wells/condition.

(D) GPR40 reporter assay in HEK293 cells treated with either DMSO or 9-PAHSA with GW1100. n = 3/condition.

(E) Calcium flux assay in mGPR40 stably transfected cells treated with DMSO, linoleic acid, 9-PAHSA, or GW1100. n = 3/condition. *$p < 0.05$ versus buffer and $^{\#}p < 0.05$ versus linoleic acid and 9-PAHSA alone.

(F) cAMP assay in mGPR40 stably transfected cells in presence of DMSO, cAMP agonist control, or 9-PAHSA. n = 3/condition. *$p < 0.05$ versus all other conditions.

(G and H) Five hours after food removal, PAHSA-treated mice were intraperitoneally injected with DMSO or DC260126 followed by insulin intraperitoneal injection or oral glucose after 30 min for an ITT (G) or OGTT (H). For (G) and (H), *$p < 0.05$ versus PAHSA+DMSO group.

(I) Glycemia, insulin, and GLP-1 levels were measured in PAHSA-treated mice before and 5 min after glucose gavage. n = 8–10/group.

*$p < 0.05$ versus baseline within same treatment, $^{\#}p < 0.05$ versus vehicle DMSO at same time point. Statistical significance was evaluated by unpaired one-tailed Student's t test or two-way ANOVA with Tukey post hoc tests. Data are means ± SEM.

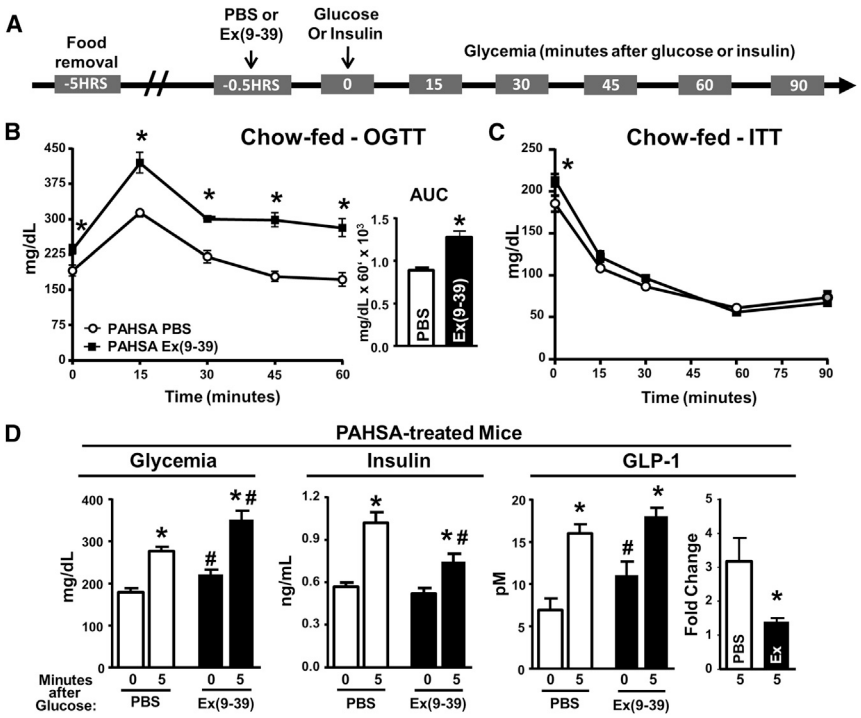

Figure 3. GLP-1R Blockade Reverses the Effect of 5- and 9-PAHSAs on Improved Glucose Tolerance

(A–C) Five hours after food removal, PAHSA-treated mice were injected intraperitoneally with either PBS or 5 μg Ex(9–39) (A) followed 30 min later by OGTT (B) or ITT (C). n = 14–16/group. *p < 0.05 versus PAHSA PBS.

(D) Glycemia, insulin, and GLP-1 levels were measured in PAHSA-treated mice before and 5 min after glucose gavage. n = 8–10/group. Ex indicates Ex(9–39). *p < 0.05 versus baseline within same treatment, #p < 0.05 versus vehicle PBS at same time point. Statistical significance was evaluated by unpaired two-tailed Student's t test or two-way ANOVA with Tukey post hoc tests. Data are means ± SEM.

treatment attenuated the PAHSA-mediated increase in GSIS. Ex(9–39) increased baseline GLP-1 levels but attenuated the increase in GLP-1 secretion above baseline in response to glucose (Figure 3D). In vehicle-treated mice, Ex(9–39) had no effect on baseline glucose (30 min after Ex(9–39)) or on glucose tolerance except at 45 min after glucose administration (Figure S3B). There was also no effect of Ex(9–39) on insulin sensitivity or on glycemia at baseline or 5 min post-glucose administration (Figures S3C and S3D). Furthermore, GLP-1R antagonism in vehicle-treated mice increased glucose-stimulated insulin and GLP-1 secretion (Figure S3D). This increase in GLP-1 secretion may be a compensatory response to GLP-1R blockade and likely stimulates insulin secretion. As expected, PAHSAs do not directly activate GLP-1R (Figure S3E), which is activated by peptides (GLP-1), not lipids. These data indicate that GLP-1 action is necessary for the full effects of PAHSAs on glucose tolerance, but not insulin sensitivity, and this may be due to PAHSA-mediated induction of GLP-1 secretion. These observations are consistent with a study in T2D people, in whom GLP-1 improves glycemic control by increasing insulin secretion and inhibiting glucagon secretion without improving insulin sensitivity (Vella et al., 2000).

Chronic PAHSA Treatment Improves Insulin Sensitivity and Glucose Tolerance, and Reduces Adipose Tissue Inflammation in HFD Mice without Altering Food Intake or Adiposity

9-PAHSA treatment for 15–18 weeks via subcutaneous minipumps in HFD mice did not alter body weight, fat mass, lean mass, food intake, serum triglycerides, or FFA levels (Figures 4A, S4A, and S4B).

9-PAHSA levels were elevated ~2-fold in serum and liver (Figure 4B) and ~33%–42% in PG and SQ WAT compared with vehicle-treated HFD mice. 9-PAHSA levels were restored to chow mouse levels in serum and PG WAT but were not completely restored in SQ WAT (Figures 4B and 1B). Chronic PAHSA treatment in HFD mice improved insulin sensitivity (Figures 4C and S4C–S4F) and glucose tolerance (Figures 4D and S4E) compared with vehicle-treated HFD mice, and these effects were sustained for at least 4.5 months. We found that 9-PAHSA treatment (12 mg/kg/day) was more effective than a split dose of 5- and 9-PAHSA (6 mg/kg of each) in HFD mice (data not shown), although the combined treatment consistently lowered glycemia 5 hr after food removal (Figure S4D). Further studies showed 9-PAHSA lowered glycemia at 5 min post-glucose in HFD mice compared with vehicle-treated HFD mice with similar insulin levels (Figure 4E), supporting enhanced insulin sensitivity. Also in support of this, chronic 9-PAHSA treatment in HFD mice prevented the increase in islet mass seen in vehicle HFD mice (Figure 4F). This suggests that the same insulin levels are more efficient in lowering glucose in PAHSA HFD mice and that expansion of islet mass is not necessary. In contrast to PAHSA-treated chow mice (Figure 1E), PAHSA treatment in HFD mice did not enhance glucose-stimulated insulin or GLP-1 secretion compared with vehicle HFD mice (Figure 4E), but similar insulin levels lowered glucose more in PAHSA HFD mice. Thus, the beneficial PAHSA effects on glucose homeostasis in HFD mice are independent of changes in glucose-stimulated insulin or GLP-1 secretion and appear to involve increased insulin sensitivity. Expression of *tnf-α* in PG WAT was lower in PAHSA-treated HFD mice compared with vehicle-treated HFD mice (Figure 4G). This indicates that reduced WAT inflammation may contribute to the enhanced glucose homeostasis in PAHSA-treated HFD mice. Overall, the beneficial effects of PAHSAs are more moderate in HFD mice than in chow mice. This may be in part due to lack of full restoration of SQ WAT PAHSA levels.

Since PAHSA beneficial effects on glucose homeostasis in chow mice are in part mediated by GPR40 (Figures 2G and 2H), we studied the role of GPR40 in mediating PAHSA effects in HFD mice. DC260126, a GPR40 antagonist, reversed PAHSA improvements on insulin (ITT) and glucose tolerance tests (GTT)

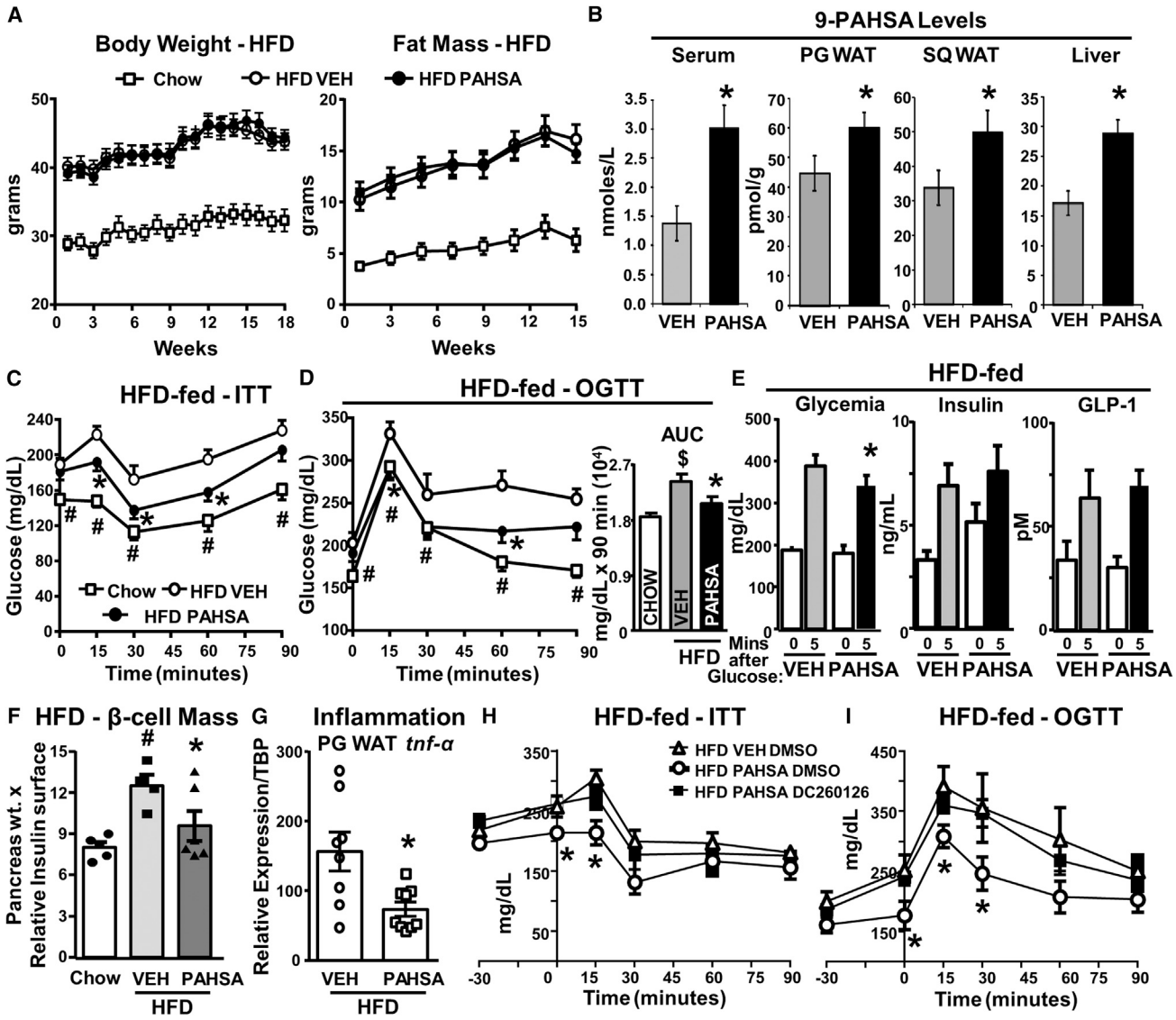

Figure 4. Chronic PAHSA Treatment Improves Insulin Sensitivity and Glucose Tolerance, and Reduces Adipose Tissue Inflammation in HFD Mice without Altering Food Intake or Adiposity

(A) Body weight and fat mass in chow-fed and HFD mice treated with 9-PAHSA via minipumps. n = 16/group.

(B) 9-PAHSA levels in sera and tissues after 4.5 months of 9-PAHSA treatment. n = 5–6/group.

(C and D) ITT (98 days of treatment; C) and OGTT (57 days of treatment; D) in vehicle and PAHSA HFD mice. Area under the curve for OGTT. n = 8–14/group. For (B), *p < 0.05 versus vehicle (VEH). For (C), *p < 0.05 versus HFD vehicle and chow, #p < 0.05 versus HFD vehicle and HFD PAHSA. For (D), *p < 0.05 HFD PAHSA versus HFD vehicle, #p < 0.05 chow versus HFD vehicle, $p < 0.05 versus chow and HFD PAHSA.

(E) Serum glucose, insulin, and GLP-1 levels 5 min post-glucose challenge in vehicle and PAHSA HFD mice after 70 days of treatment. n = 7–8/group. *p < 0.05 versus vehicle at same time point.

(F) β cell mass quantification (n = 2–3 sections/mouse, 4–6 mice/group). *p < 0.05 versus HFD vehicle; #p < 0.05 versus chow.

(G–I) PG WAT *tnf-α* expression (G) in vehicle and PAHSA HFD mice. n = 8–9/group. *p < 0.05 versus HFD vehicle. Five hours after food removal, PAHSA-treated mice were injected intraperitoneally with DMSO or DC260126 followed 30 min later by ITT (H) or OGTT (I). n = 5–6/group.

For (H) and (I), *p < 0.05 versus HFD vehicle DMSO and HFD PAHSA DC260126. Statistical significance was evaluated by unpaired one-tailed Student's t test or two-way ANOVA with Tukey post hoc tests. Data are means ± SEM.

in HFD mice (Figures 4H and 4I), but had no effect in vehicle HFD mice (Figures S4E and S4F). This effect of GPR40 inhibition in PAHSA HFD mice is mainly due to reversing PAHSA effects on lowering glycemia at time "0 min" of the oral GTT (OGTT) and ITT (Figures 4H, 4I, S4G, and S4H). These data suggest that GPR40 mediates at least some of the beneficial effects of PAHSAs in HFD mice, similar to the effects in chow mice.

Prior to this study, we had investigated only acute effects of PAHSAs on glucose homeostasis, primarily with a single dose (Yore et al., 2014). Furthermore, we did not report data on insulin sensitivity. A major advance of this study is demonstrating that

PAHSAs enhance insulin sensitivity. This is important because there is a major unmet medical need for safe insulin-sensitizing agents. Currently there are no anti-diabetic drugs that are primarily insulin-sensitizing except thiazolidinediones, which have adverse effects. Safe insulin-sensitizing agents could be used to prevent and treat insulin resistance, T2D, and cardiovascular complications.

Since serum PAHSA levels correlate highly with insulin sensitivity in humans, and PAHSA levels are reduced in serum and SQ WAT of insulin-resistant people and HFD mice, we designed the current study to restore circulating and tissue PAHSA levels within the physiologic range (Yore et al., 2014). Although we achieved this in chow mice and in serum and PG WAT of HFD mice, we did not fully restore levels in SQ WAT of HFD mice. This could contribute to the more modest effects on insulin sensitivity and glucose tolerance in HFD mice. The effects are also greater in chow mice with a mixed genetic background (Figures 1F–1I), which is more relevant to human disease than inbred C57BL/6 mice. Future studies will investigate the effects of PAHSA treatment in HFD mice on a mixed genetic background.

Another major advance is that we identified a new receptor that is directly activated by PAHSAs, GPR40. GPR40 blockade in chow mice attenuates PAHSA-mediated improvements in glucose tolerance, insulin sensitivity, and GSIS, but not glucose-stimulated GLP-1 secretion. The fact that PAHSAs have direct effects on insulin secretion independent of GLP-1 as well as GLP-1-dependent effects is supported by our data showing they stimulate GSIS in isolated human islets (Figure 2A). GLP-1R plays a role in some, but not all, PAHSA effects in chow mice since GLP-1R blockade attenuates PAHSA-mediated improvements in glucose tolerance, but not insulin sensitivity. In HFD mice, GPR40 blockade attenuates PAHSA-mediated beneficial effects on glucose tolerance and systemic insulin sensitivity. These observations do not eliminate a role for GPR120 that could mediate the PAHSA effects on GLP-1 secretion, glucose uptake, and some anti-inflammatory effects (Yore et al., 2014; Lee et al., 2016).

In sum, this study expands our understanding of PAHSA biology by demonstrating sustained beneficial effects of chronic treatment without tachyphylaxis or islet exhaustion. In fact, PAHSAs appear to enhance islet function in HFD mice since expansion of islet mass, which we observe in vehicle-treated HFD mice, is prevented by PAHSA treatment. Yet the islets produce the same amount of insulin and lower glycemia more in PAHSA-treated HFD mice than in vehicle-treated HFD mice. PAHSA-mediated beneficial effects are achieved with subcutaneous delivery via minipumps, indicating that the oral route is not necessary for PAHSA effects on glucose homeostasis. These sustained effects of PAHSAs are in part mediated by GPR40. Because PAHSAs can activate multiple GPCRs, which are known to mediate beneficial metabolic effects, and PAHSA levels are reduced in insulin-resistant people, restoring PAHSA levels has high therapeutic potential to prevent and/or treat T2D.

Study Limitations

These studies clearly demonstrate that chronic treatment of chow-fed and HFD-fed mice with PAHSAs enhances insulin sensitivity and glucose tolerance and reduces adipose inflammation. Furthermore, PAHSAs activate GPR40, which mediates some of their beneficial effects. Nevertheless, these studies have some limitations. Although we and others (Hu et al., 2009) tested the specificity of the GPR40 inhibitor, DC260126, in assays with several other GPCRs including another receptor of the same subtype, $G_{\alpha q/11}$, it is still possible that there could be off-target effects of this inhibitor. The fact that DC260126 does not have effects on OGTT or ITT in vehicle-treated mice makes this less of a concern. The observation that DC260126 lowers baseline insulinemia in PAHSA-treated mice and impairs GSIS (as well as the augmentation of insulin secretion by PAHSA treatment) may be unexpected, since GPR40 mediates fatty acid-activated insulin secretion, but generally not glucose-activated insulin secretion. But DC260126 inhibits the rise in intracellular Ca^{+2} levels in response to fatty acids (Hu et al., 2009). Since PAHSAs are delivered constantly by minipump, DC260126 may be reducing intracellular Ca^{+2} even in the basal state (i.e., before glucose administration), thereby lowering baseline insulinemia. In addition, DC260126 may inhibit an increase in intracellular Ca^{2+} elicited by glucose or other insulin secretagogues in islet β cells. Another mechanism for the effects of DC260126 on GSIS is that small-molecule inhibitors can bind to GPCRs like GPR40 in a fashion that modulates their baseline activity (Milligan et al., 2017). Future experiments in which we can conditionally knock down GPR40 in adult mice in a tissue-specific manner will be useful to investigate these mechanisms. Despite these caveats, the facts that genetic knockdown of GPR40 in a β cell line and that a different GPR40 inhibitor directly blocks PAHSA potentiation of insulin secretion in human islets support our conclusion that PAHSA effects on insulin secretion are mediated by GPR40.

STAR★METHODS

Detailed methods are provided in the online version of this paper and include the following:

- KEY RESOURCES TABLE
- CONTACT FOR REAGENT AND RESOURCE SHARING
- EXPERIMENTAL MODEL AND SUBJECT DETAILS
  - Mice and Husbandry Conditions
  - Cell Culture
- METHOD DETAILS
  - Measurement of Metabolic Parameters
  - PAHSA Extraction and Measurements
  - Anti-Inflammatory Effects of PAHSAs
  - GPR40 Receptor Reporter Assay
  - GLP-1 Receptor Reporter Assay
  - Ca^{2+} Measurements – Multispan
  - Cyclic AMP Assay – Multispan
  - Glucose-Stimulated Insulin Secretion in Human Islets
  - GLP-1 Secretion from Enteroendocrine STC-1 Cells
  - Determination of β-Cell Mass
  - Quantitative PCR
  - Analytical Procedures
- QUANTIFICATION AND STATISTICAL ANALYSIS

SUPPLEMENTAL INFORMATION

Supplemental Information includes four figures and can be found with this article online at https://doi.org/10.1016/j.cmet.2018.01.001.

ACKNOWLEDGMENTS

We thank Dr. Ji Lei, the director of BADERC Pancreatic Islet Core (NIH P30 DK57521), for providing human islets, and Dr. Douglas Hanahan for the STC-1 cells. We thank Dr. Susan Bonner-Weir, Director of the Joslin DRC Advanced Microscopy Core (NIH P30 DK036836), from the Joslin Diabetes Center for her expertise and conversations related to islet biology analyses. The Harvard Digestive Disease Center Core B (NIH P30DK034854) processed and immunostained samples. Imaging was performed at the Neuro Imaging Facility (NINDS P30 Core Center) for islet mass quantification. Supported by NIH grants R01 DK43051, P30 DK57521 (B.B.K.), and R01 DK106210 (B.B.K. and A. Saghatelian); a grant from the JPB Foundation (B.B.K.); and T32DK07516 (B.B.K. and J.L.).

AUTHOR CONTRIBUTIONS

I.S. and J.L. conceived, designed, performed, and interpreted experiments and made figures. P.M.M.-V. designed, performed, and interpreted the immunology experiments and made the figures. C.J.D., A. Saghatelian, and B.B.K. designed and performed the receptor activation experiments. M.J.K. performed the uptake studies. A.T.N., D.S., and A. Saghatelian designed and performed chemical synthesis of the lipids. A. Sontheimer, P.A., O.D.P., K.W., and J.J.Z. assisted with animal studies. J.M. and I.S.F. participated in interpreting results of GPR40 assays. M.M.Y. designed and performed GLP-1 assay *in vitro*. B.B.K. and A. Saghatelian conceived, designed, and supervised the experimental plan and interpreted experiments. B.B.K., I.S., and J.L. wrote the manuscript. A. Saghatelian and P.M.M.-V. edited the manuscript.

DECLARATION OF INTERESTS

I.S., J.L., P.M.M.-V., M.M.Y., A. Saghatelian, and B.B.K. are inventors on patents related to the PAHSAs: patent #WO2013166431A1 and patent #WO2017070515A3.

Received: August 15, 2016
Revised: August 24, 2017
Accepted: January 3, 2018
Published: February 6, 2018

REFERENCES

Aroda, V.R., Henry, R.R., Han, J., Huang, W., DeYoung, M.B., Darsow, T., and Hoogwerf, B.J. (2012). Efficacy of GLP-1R agonists and DPP-4 inhibitors: meta-analysis and systematic review. Clin. Ther. *34*, 1247–1258.e22.

Ayala, J.E., Bracy, D.P., James, F.D., Julien, B.M., Wasserman, D.H., and Drucker, D.J. (2009). The glucagon-like peptide-1 receptor regulates endogenous glucose production and muscle glucose uptake independent of its incretin action. Endocrinology *150*, 1155–1164.

Bruce, D.G., Storlien, L.H., Furler, S.M., and Chisholm, D.J. (1987). Cephalic phase metabolic responses in normal weight adults. Metabolism *36*, 721–725.

Burant, C.F., Viswanathan, P., Marcinak, J., Cao, C., Vakilynejad, M., Xie, B., and Leifke, E. (2012). TAK-875 versus placebo or glimepiride in T2D mellitus: a phase 2, randomised, double-blind, placebo-controlled trial. Lancet *379*, 1403–1411.

Campbell, J.E., and Drucker, D.J. (2013). Pharmacology physiology and mechanisms of incretin hormone action. Cell Metab. *17*, 819–837.

Christensen, L.W., Kuhre, R.E., Janus, C., Svendsen, B., and Holst, J.J. (2015). Vascular, but not luminal, activation of FFAR1 (GPR40) stimulates GLP-1 secretion from isolated perfused rat small intestine. Physiol. Rep. *3*, e12551.

Edfalk, S., Steneberg, P., and Edlund, H. (2008). Gpr40 is expressed in enteroendocrine cells and mediates free fatty acid stimulation of incretin secretion. Diabetes *57*, 2280–2287.

Holst, J.J. (2007). The physiology of glucagon-like peptide 1. Physiol. Rev. *87*, 1409–1439.

Hu, H., He, L.Y., Gong, Z., Li, N., Lu, Y.N., Zhai, Q.W., Liu, H., Jiang, H.L., Zhu, W.L., and Wang, H.Y. (2009). A novel class of antagonists for the FFAs receptor GPR40. Biochem. Biophys. Res. Commun. *390*, 557–563.

International Diabetes Federation. (2013). IDF Diabetes Atlas, Sixth Edition (International Diabetes Federation).

Iglesias, J., Barg, S., Vallois, D., Lahiri, S., Roger, C., Yessoufou, A., Pradevand, S., McDonald, A., Bonal, C., Reimann, F., et al. (2012). PPARβ/δ affects pancreatic β-cell mass and insulin secretion in mice. J. Clin. Invest. *122*, 4105–4117.

Itoh, Y., Kawamata, Y., Harada, M., Kobayashi, M., Fujii, R., Fukusumi, S., Ogi, K., Hosoya, M., Tanaka, Y., Uejima, H., et al. (2003). Free fatty acids regulate insulin secretion from pancreatic beta cells through GPR40. Nature *422*, 173–176.

Kowluru, A., Veluthakal, R., Rhodes, C.J., Kamath, V., Syed, I., and Koch, B.J. (2010). Protein farnesylation-dependent Raf/extracellular signal-related kinase signaling links to cytoskeletal remodeling to facilitate glucose-induced insulin secretion in pancreatic β-cells. Diabetes *59*, 967–977.

Lee, J., Moraes-Vieira, P.M., Castoldi, A., Aryal, P., Yee, E.U., Vickers, C., Parnas, O., Donaldson, C.J., Saghatelian, A., and Kahn, B.B. (2016). Branched fatty acid esters of hydroxy fatty acids (FAHFAs) protect against colitis by regulating gut innate and adaptive immune responses. J. Biol. Chem. *291*, 22207–22217.

Leifke, E., Naik, H., Wu, J., Viswanathan, P., Demanno, D., Kipnes, M., and Vakilynejad, M. (2012). A multiple ascending-dose study to evaluate safety, pharmacokinetics, and pharmacodynamics of a novel GPR40 agonist, TAK-875, in subjects with type 2 diabetes. Clin. Pharmacol. Ther. *92*, 29–39.

Luzi, L., and DeFronzo, R.A. (1989). Effect of loss of first-phase insulin secretion on hepatic glucose production and tissue glucose disposal in humans. Am. J. Physiol. *257*, E241–E246.

Ma, Y., Kind, T., Vaniya, A., Gennity, I., Fahrmann, J.F., and Fiehn, O. (2015). An in silico MS/MS library for automatic annotation of novel FAHFA lipids. J. Cheminform. *7*, 53.

Meier, J.J. (2012). GLP-1 receptor agonists for individualized treatment of type 2 diabetes mellitus. Nat. Rev. Endocrinol. *8*, 728–742.

Milligan, G., Shimpukade, B., Ulven, T., and Hudson, B.D. (2017). Complex pharmacology of free fatty acid receptors. Chem. Rev. *117*, 67–110.

Moraes-Vieira, P.M., Yore, M.M., Dwyer, P.M., Syed, I., Aryal, P., and Kahn, B.B. (2014). RBP4 activates antigen-presenting cells, leading to adipose tissue inflammation and systemic insulin resistance. Cell Metab. *19*, 512–526.

Steneberg, P., Rubins, N., Bartoov-Shifman, R., Walker, M.D., and Edlund, H. (2005). The FFA receptor GPR40 links hyperinsulinemia, hepatic steatosis, and impaired glucose homeostasis in mouse. Cell Metab. *1*, 245–258.

Vella, A., Shah, P., Basu, R., Basu, A., Holst, J.J., and Rizza, R.A. (2000). Effect of glucagon-like peptide 1(7-36) amide on glucose effectiveness and insulin action in people with type 2 diabetes. Diabetes *49*, 611–617.

Villanueva-Peñacarrillo, M.L., Martín-Duce, A., Ramos-Álvarez, I., Gutiérrez-Rojas, I., Moreno, P., Nuche-Berenguer, B., Acitores, A., Sancho, V., Valverde, I., and González, N. (2011). Characteristic of GLP-1 effects on glucose metabolism in human skeletal muscle from obese patients. Regul. Pept. *168*, 39–44.

Yore, M.M., Syed, I., Moraes-Vieira, P.M., Zhang, T., Herman, M.A., Homan, E.A., Patel, R.T., Lee, J., Chen, S., Peroni, O.D., et al. (2014). Discovery of a class of endogenous mammalian lipids with anti-diabetic and anti-inflammatory effects. Cell *159*, 318–332.

Zhang, T., Chen, S., Syed, I., Ståhlman, M., Kolar, M.J., Homan, E.A., Chu, Q., Smith, U., Borén, J., Kahn, B.B., et al. (2016). A LC-MS–based workflow for measurement of branched fatty acid esters of hydroxy fatty acids. Nat. Protoc. *11*, 747–763.

STAR★METHODS

KEY RESOURCES TABLE

REAGENT or RESOURCE	SOURCE	IDENTIFIER
Antibodies		
CD11c+ (PE)	Biolegend	BioLegend Cat# 117308, RRID: AB_313777
CD206+ (APC)	Biolegend	BioLegend Cat# 141708, RRID: AB_10900231
IL-1β (PE)	E-bioscience	Thermo Fisher Scientific Cat# 12-7114-80, RRID: AB_10736472
TNFα (PE-Cy7)	Biolegend	BioLegend Cat# 506324, RRID: AB_2256076
Gr1 (LY6C/LY6G) – (PE-Cy7)	Biolegend	BioLegend Cat# 108415, RRID: AB_313380
MHCII (Alexa 700)	Biolegend	BioLegend Cat# 107622, RRID: AB_49372
Ly6G (Perp Cy5)	Biolegend	BioLegend Cat# 127616, RRID: AB_1877271
Ly6C (PE-Cy7)	Biolegend	BioLegend Cat# 128017, RRID: AB_1732093
F4/80 (Pacific blue)	Biolegend	122612
CD11b (APC-Cy7)	Biolegend	BioLegend Cat# 101226, RRID: AB_830642
CD45 (Brilliant Violet (500))	BD bioscience	BD Biosciences Cat# 561487, RRID: AB_10697046
Chemicals, Peptides, and Recombinant Proteins		
HumulinR	Lilly	NDC0002-8215-01
Exendin (9-39)	Bachem	H-8740
DC260126	Tocris	5357
GW1100	Cayman Chemical	306974-70-9
Linoleic Acid	Sigma-Aldrich	L1376
GLP-1	Sigma-Aldrich	SCP0153
5-PAHSA (racemic mixture)	Siegel and Saghatelian labs	Yore et al., 2014
9-PAHSA (racemic mixture)	Siegel and Saghatelian labs	Yore et al., 2014
Hydroxy Stearic Acid	Siegel lab	Yore et al., 2014
D-(+)glucose	Sigma-Aldrich	G8270
Palmitate	Sigma-Aldrich	P9767
Bovine serum albumin (BSA)	Sigma-Aldrich	A4503
Phosphate buffered saline (PBS)	Sigma-Aldrich	P5368
Dimethyl sulfoxide (DMSO)	Sigma-Aldrich	D8418
Tween-80	Sigma-Aldrich	P4780
PEG-400	Sigma-Aldrich	81172
Krebs-Ringer Bicarbonate buffer	Sigma-Aldrich	K4002
Phorbol-12-myristate-13-acetate (PMA)	Sigma-Aldrich	P8139
Ionomycin	Sigma-Aldrich	I9657
Brefeldin A	Sigma-Aldrich	B7651
Calcium dye loading buffer	Multispan	MSCA01-1
Lipofectamine2000	Thermo Fisher Scientific	11668027
Methanol	Honeywell Burdick & Jackson	A456-4
Chloroform	Honeywell Burdick & Jackson	BJGC049-4
Citric acid	Sigma-Aldrich	5330010050
Critical Commercial Assays		
Insulin (mouse, ELISA)	Crystal Chem	90080
Insulin (human, ELISA)	Alpco Diagnostics	80-INSHU-E01.1
GLP-1, total (mouse, ELISA)	Millipore	EZGLP1T-36K
Triglycerides	Pointe Scientific	T7532
Free fatty acids (FFA), Color Reagent A	Wako Diagnostics	999-34691

(*Continued on next page*)

Continued		
REAGENT or RESOURCE	SOURCE	IDENTIFIER
FFA, Solvent A	Wako Diagnostics	995-34791
FFA, Color Reagent B	Wako Diagnostics	991-34891
FFA, Solvent B	Wako Diagnostics	993-35191
FLIPR 384	Molecular Devices	Multispan
HTRF cAMP HiRange Kit	CisBio	Multispan
Experimental Models: Cell Lines		
MIN6 cells	ATTC	CRL-11506
STC-1 cells	ATTC	CRL-3254
HEK293T cells	ATTC	CRL-11268
Experimental Models: Organisms/Strains		
Mouse: C57BL/6J	Jackson labs	000664
Mouse: C57BL/6J & FVB mixed background	BIDMC Animal Facility	In-house breeding
Human Islets	BADERC Islet Core Facility, Massachusetts General Hospital	Donor bank
Oligonucleotides		
tnfα	IDT	Custom
gpr40	IDT	Custom
SYBR Green PCR Master Mix	Life Technologies	4309155
Advantage RT-for-PCR kit, 100 reactions	Clontech	639506
Recombinant DNA		
GPR40 siRNA	Thermo Fisher Scientific	s107455, s107454, s202585
Software and Algorithms		
GraphPad	GraphPad Software	https://www.graphpad.com/
Fiji	NIH	https://fiji.sc
Other		
Subcutaneous minipumps	Alzet	Model 2006
Chow	Purina Lab Diet	5008
High fat diet	Harlan Teklad	93075

CONTACT FOR REAGENT AND RESOURCE SHARING

Further information and request for resources and reagents should be directed to and will be fulfilled by the Lead Contact, Barbara B. Kahn (bkahn@bidmc.harvard.edu).

EXPERIMENTAL MODEL AND SUBJECT DETAILS

Mice and Husbandry Conditions

Chow-fed (Purina Lab diet, 5008) male C57Bl/6J wild-type mice (Jackson Laboratories) and in-house bred mixed background mice (C57Bl/6J and FVB) were randomized to treatment group based on body weight at 8 wks of age and implanted with subcutaneous minipumps (Alzet, Model2006). Similarly, randomized male C57Bl/6J wild-type mice were placed on HFD (Research Diets, Td93075) at 6 wks of age. After 8 weeks on HFD, insulin resistance was confirmed by an insulin tolerance test (ITT). Minipumps were implanted after 9 weeks on HFD. All mice were singly housed in ventilated cages with ad libitum access to food and water. Mice were kept on a 14 hr light, 10 hr dark schedule at 22-23°C. All animal care and use procedures were in accordance with and approved by the Institutional Animal Care and Use Committee at Beth Israel Deaconess Medical Center, Boston, MA.

Cell Culture

MIN6 cells obtained from ATCC (animals of unknown gender) were maintained at 37°C and cultured in RPMI 1640 medium containing 10 % heat-inactivated fetal bovine serum supplemented with 100 IU/ml penicillin and 100 IU/ml streptomycin, 1 mM sodium pyruvate, 50 μM 2-mercaptoethanol, and 10 mM HEPES [pH 7.4]. The medium was changed twice and cells were subcloned weekly. Endogenous GPR40 expression was depleted by transfecting MIN6 cells using a pool of GPR40 siRNA at a final concentration of 100 nmol/l using Lipofectamine transfection reagent. To assess the specificity of RNA interference method, cells were transfected with non-targeting RNA i.e., scrambled RNA. Efficiency of GPR40 knockdown was determined by qPCR.

STC-1 and HEK293T cells obtained from ATCC were maintained in DMEM supplemented with 10% FCS, 100 IU/ml penicillin and 100 IU/ml streptomycin, and maintained at 37°C and 5% CO2.

Human islets from normal donors obtained from BADERC Islet Core Facility, Massachusetts General Hospital, were cultured in human islet media with 100 IU/ml penicillin and 100 IU/ml streptomycin, and maintained at 37°C and 5% CO2.

METHOD DETAILS

Measurement of Metabolic Parameters

Minipumps filled with either vehicle (50% PEG-400, 0.5% Tween-80, 49.5% distilled water) or 5- and 9-PAHSAs (Chow: 2mg/kg of each; HFD: 6mg/kg of each or 12mg/kg of 9-PAHSA) or 4mg/kg of palmitate were inserted subcutaneously in 8-wk-old chow and 15-wk-old HFD mice. For in vivo studies, the GLP-1R antagonist, Ex(9-39) (5μg/mouse) and the GPR40 antagonist, DC260126 (5mg/kg; Tocris Bioscience) were administered intraperitoneally. Body weight and food intake were measured weekly and body composition measured by MRI. Insulin tolerance test (ITT) and oral glucose tolerance test (OGTT) were performed as described (Yore et al., 2014) following 5 hr. food removal. 4.5 hr. after food removal (0.5 hr. before initiation of the OGTT or ITT) mice were intraperitoneally injected with either GLP-1 receptor antagonist, Exendin (9-39) or GPR40 antagonist, DC260126. Mice received 1 g/Kg glucose by gavage or 0.5-0.7 IU of insulin intraperitoneally 30 min after antagonist administration and glycemia was monitored over a 2 hr. period. For glucose-stimulated insulin and GLP-1 secretion studies, mice were bled at t=0 (baseline) and 5 min post glucose gavage from the tail vein and blood was transferred into tubes and serum insulin and total GLP-1 levels were measured by ELISA. At the end of the study, mice were sacrificed by decapitation for serum collection and tissues were harvested, snap frozen in liquid nitrogen and stored at -80°C until further processed.

PAHSA Extraction and Measurements

Lipid extraction was performed as described (Yore et al., 2014). Tissues (60-100mg) were Dounce homogenized on ice in a mixture of 1.5mL MeOH, 1.5mL chloroform and 3mL citric acid buffer. PAHSA standards were added to chloroform prior to extraction. The final mixture was centrifuged and the organic phase containing was dried under N_2 and stored at -80°C prior to solid phase extraction (Yore et al., 2014; Zhang et al., 2016).

Anti-Inflammatory Effects of PAHSAs

PG WAT stromal vascular fraction cells were harvested and surface markers were stained with monoclonal antibodies (Biolegend, E-Bioscience, BD bioscience) for multicolor flow cytometry. Intracellular cytokines were measured as previously described (Moraes-Vieira et al., 2014). In brief, SVFs were stimulated *in vitro* for 5 h at 37° C in 5% CO_2 with phorbol-12-myristate-13-acetate (PMA; 100 ng/mL), ionomycin (1 μg/mL) and brefeldin A (1 μg/mL) (Sigma-Aldrich, St. Louis, MO, USA). Cells were washed and stained with specific antibodies for surface molecules (CD11b, CD45, CD11c, CD206, F4/80) (Biolegend) and permeabilized using the BD Cytofix/Cytoperm Fixation/Permeabilization solution kit (BD Biosciences, San Jose, CA, USA). Intracellular staining was performed with PE-Cy7-conjugated anti-TNF (Biolegend) and PE-conjugated anti-IL-1beta (eBioscience) antibodies. Cells were acquired with an LSR II flow cytometer (BD) and analyzed by FlowJo software.

GPR40 Receptor Reporter Assay

HEK293T cells were transfected with GPR40 and SRE-luc 44-235 and treated with DMSO control, 5-PAHSA (100μM), or 9-PAHSA (0-100μM) with or without GW1100 (0-10μM). At the end of the treatment luciferase activity was measured and relative luciferase units were calculated.

GLP-1 Receptor Reporter Assay

HEK293T cells were transfected with GLP-1 and CRE-luc and treated with DMSO control, 5-PAHSA (20 and 100μM), or 9-PAHSA (20 and 100μM), hydroxystearic acid (100μM), sodium palmitate (100μM) and GLP-1 (10pM). At the end of the treatment luciferase activity was measured and relative luciferase units were calculated.

Ca^{2+} Measurements – Multispan

Multispan's mouse GPR40 stable cell line, HEK293T cells were grown in DMEM, 10% FBS, and 1 μg/mL puromycin. On the day of assay, cells were lifted with non-enzymatic cell stripper and seeded in 384-well poly-d-lysine coated plate in assay buffer (HBSS + 20mM HEPES) at an appropriate density. The calcium dye loading buffer (Multispan, Cat# MSCA01-1) was added to cells and incubated for 30 minutes at 37°C followed by 30 minutes at room temperature. In antagonist mode, cells were pre-incubated with GW1100 for 15 minutes at room temperature prior to the addition of 9-PAHSA at 100mM concentration. Calcium flux was monitored for 180 sec with 9-PAHSA injected into the well at the 19th second read by FLIPR 384 (Molecular Devices).

Cyclic AMP Assay – Multispan

Cells were lifted with non-enzymatic cell stripper and resuspended in assay buffer at desired concentrations. cAMP assays were performed according to the manufacturer's protocol using CisBio's HTRF cAMP HiRange Kit. Cells were incubated with compounds for 30 minutes at 37°C. The reaction was terminated by sequentially adding D2-labeled cAMP and cryptate-labeled anti-cAMP antibody

in lysis buffer. The plate was incubated at room temperature for 60 minutes before reading fluorescent emissions at 620 nm and 668 nm with excitation at 314 nm on FlexStation III (Molecular Devices). Cyclic AMP assay results are shown as "Ratio 668/620 x 10,000" (ratio of fluorescence at 668 nm and 620 nm x 10,000). Data in graphs are represented in Mean ± SD. Dose-dependent responses were fitted with sigmoidal dose-response curves allowing variable slopes using GraphPad Prism version 6. The graphs display dose-dependent stimulation of intracellular cAMP level upon treatment with control ligand or compounds.

Glucose-Stimulated Insulin Secretion in Human Islets

Human islets from normal donor were obtained from BADERC Core facility, MGH, Bosotn. GSIS was assessed as previously outlined (Kowluru et al., 2010). Briefly, human islets were cultured overnight in human islet media. Following a 2 hr incubation in Krebs-Ringer Bicarbonate buffer (KRB) with 0.5% BSA (pH 7.4), islets were stimulated with either 2.5 mM or 20 mM glucose in presence or absence of DMSO, 9-PAHSA (20μM), and GW1100 (10μM) for 45 mins at 37°C. At the end, media was collected and insulin was quantitated by ELISA (Alpco Diagnostics).

GLP-1 Secretion from Enteroendocrine STC-1 Cells

GLP-1 secretion studies were performed as previously described (Yore et al., 2014). In brief, STC-1 cells were plated in 24-well plates 72 hrs before assay initiation. Cells were washed with incubation buffer B (Hanks' balanced salt solution supplemented with 20mM HEPES) and incubated with 5- or 9-PAHSA or DMSO control at 37°C for 1 hr. Total GLP-1 measurements were performed using supernatant by ELISA (Millipore, Billerica, MA).

Determination of β-Cell Mass

Pancreata from mice treated chronically with vehicle or 9-PAHSA were fixed in 10% formalin and processed for hematoxylin and eosin staining. 2-3 full pancreas sections with 19-40 islets per section were imaged in bright field to determine β-cell mass as described (Iglesias et al., 2012). β-cell mass was calculated using the following equation: β-cell mass = pancreas weight (mg) x relative insulin surface (total islet area μm^2/total pancreas area μm^2). Relative islet surface areas were analyzed using Fiji software.

Quantitative PCR

RNA was extracted using Tri-Reagent (MRC) and cDNA was generated with random hexamers (Clontech). Quantitative real-time PCR was performed with the ABI Prism sequence detection system. Each sample was run in duplicate, and the quantity of GPR40 mRNA in each sample was normalized to mouse TATA-box binding protein (mTBP) mRNA levels. All primers were obtained from IDT DNA.

Analytical Procedures

Serum triglycerides were measured by colorimetric enzyme assay, and serum free fatty acids were measured using the NEFA-C kit (Wako, Richmond, Virginia).

QUANTIFICATION AND STATISTICAL ANALYSIS

Data are presented as means±SEM. Significance was assessed by Student's t-tests and/or ANOVA with Tukey post-test for multiple comparisons where appropriate. No data were excluded from the analyses. Statistical analysis were performed with GraphPad Prism and differences were considered significant when $p<0.05$. Statistical parameters can be found in the figure legends.

Cell Metabolism, Volume *27*

Supplemental Information

Palmitic Acid Hydroxystearic Acids Activate GPR40, Which Is Involved in Their Beneficial Effects on Glucose Homeostasis

Ismail Syed, Jennifer Lee, Pedro M. Moraes-Vieira, Cynthia J. Donaldson, Alexandra Sontheimer, Pratik Aryal, Kerry Wellenstein, Matthew J. Kolar, Andrew T. Nelson, Dionicio Siegel, Jacek Mokrosinski, I. Sadaf Farooqi, Juan Juan Zhao, Mark M. Yore, Odile D. Peroni, Alan Saghatelian, and Barbara B. Kahn

Figure S1. Related to Figure 1.

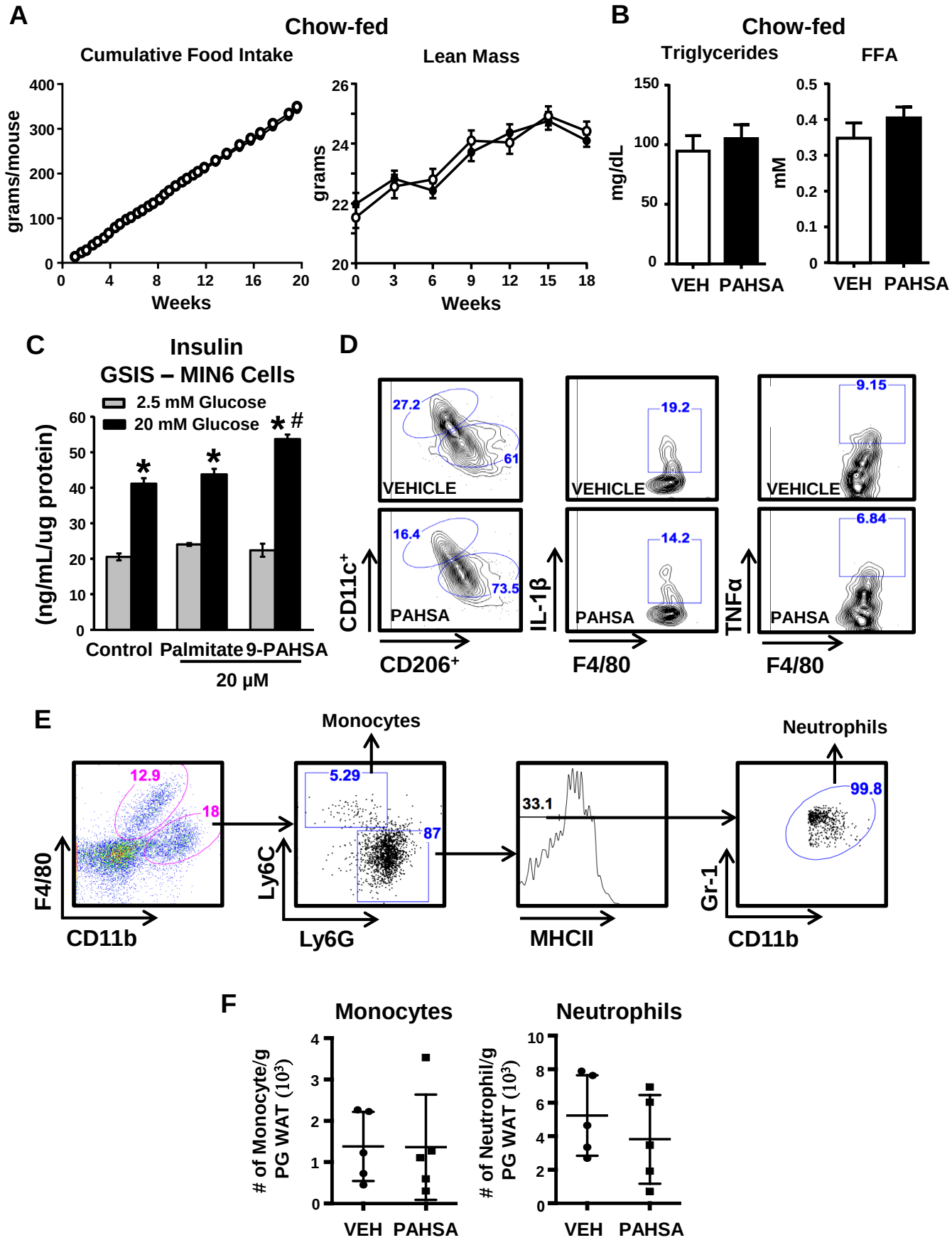

<u>Figure S1.</u> Chronic PAHSA treatment in chow-fed mice does not affect food intake, lean mass, serum triglycerides, free fatty acids or the number of PG WAT monocytes and neutrophils. Related to Figure 1.

(A) Food intake and lean mass were measured in chow-fed mice treated with vehicle or 5- and 9-PAHSA- (2 mg/kg body weight/day of each) delivered by subcutaneous minipumps for 5 months. n=16/group. (B) Serum triglycerides and free fatty acids (FFA) were measured after 5 months of treatment. Data are means±SEM. (C) Insulin secretion from MIN6 cells treated with DMSO, 9-PAHSA (20 μM), or palmitate (20 μM) for 45 minutes during glucose (20 mM) stimulation. *$p<0.05$ vs. respective 2.5mM glucose, #$p<0.05$ vs. Control 20mM glucose and palmitate. (D) Gating strategies for measuring the number of CD11c+and CD206+macrophages, and macrophages expressing IL-1β and TNF-α in PG WAT of vehicle- and PAHSA-treated mice after 5 months of treatment. (E) Gating strategies for measuring PG WAT monocytes and neutrophils from same mice as in (D). (F) The total number of PG WAT monocytes and neutrophils from vehicle and PAHSA-treated mice. n=4-5/group. Statistical significance was evaluated by unpaired two-tailed Student's t-test. Data are means±SEM.

Figure S2. Related to Figure 2.

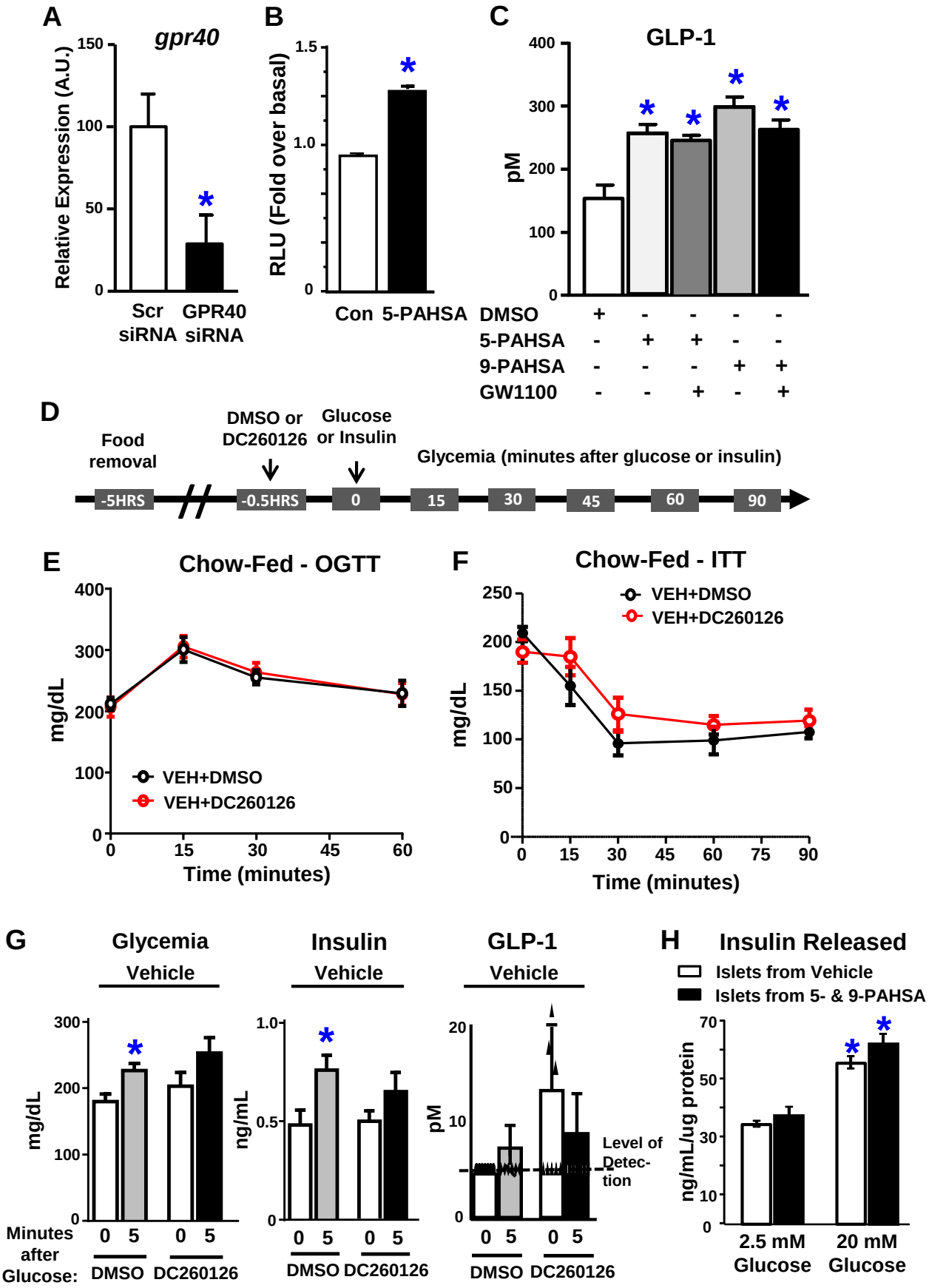

Figure S2: Effects of GPR40 antagonism on PAHSA activation of GPR40, PAHSA stimulation of GLP-1 secretion and on glucose-insulin homeostasis in vehicle-treated mice. Related to Figure 2.

(A) GRP40 mRNA expression in MIN6 cells transfected with scrambled or GPR40 siRNA. n=6 wells/condition. *p<0.05 vs. scrambled siRNA. (B) GPR40 reporter assay in HEK293 cells treated with control or 20 μM 5-PAHSA. n=3 wells/condition. *p<0.05 vs. control. (C) Total GLP-1 secretion in STC-1 cells pre-treated with 5-PAHSA or 9-PAHSA (20 μM) with or without GW1100 (10 μM) followed by acute stimulation with glucose. n=6 wells/condition, p<0.05 vs. DMSO. (D) 5-hours after food removal vehicle-treated mice were injected with either DMSO or DC260126 (5 mg/kg body weight dose) intraperitoneally followed by a glucose gavage or insulin I.P. injection after 30 minutes for an OGTT (E) or ITT (F). n=14-16/group. (G) Following the same protocol as (D), glycemia, insulin and GLP-1 levels were measured in vehicle-treated mice at baseline and 5 minutes after a glucose gavage. Most values for GLP-1 secretion were below the assay detection limit. n=14-16/group. *p<0.05 vs. baseline within same treatment. Data are means±SEM. (H) Insulin secretion in islets isolated from vehicle and PAHSA-treated mice after 5 months of treatment and stimulated with either 2.5 or 20 mM glucose. n=7 mice/group. *p<0.05 vs. 2.5mM glucose within same treatment. Statistical significance was evaluated by unpaired two-tailed Student's t-test. Data are means±SEM.

Figure S3. Related to Figure 3.

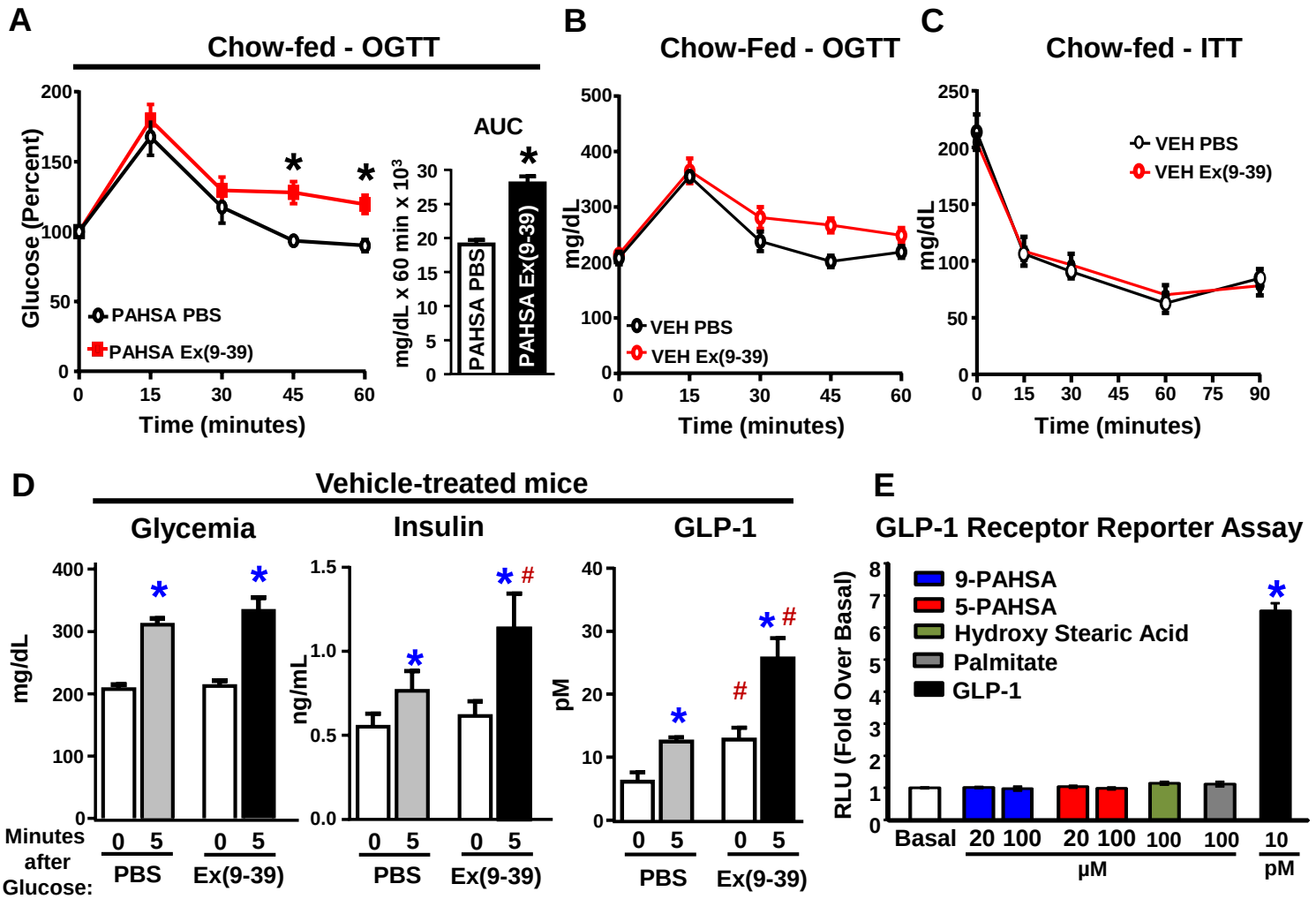

Figure S3. The GLP-1R antagonist, Exendin (9-39), reverses enhanced glucose tolerance in PAHSA-treated mice but has no effect on glucose tolerance or insulin sensitivity in vehicle-treated mice. Related to Figure 3.

(A) 5-hours after food removal, PAHSA-treated mice were injected i.p. with either PBS or 5μg Ex(9-39) 30 minutes prior to the start of an OGTT. Glucose excursion is normalized to baseline glycemia. n=14-16/group. *p<0.05 vs. PAHSA PBS. (B and C) 5-hours after food removal, vehicle-treated mice were injected with either PBS or 5μg Ex(9-39) intraperitoneally followed by glucose gavage or insulin injection i.p. after 30 minutes for an OGTT (B) or ITT (C). n=14-16/group. *p<0.05 vs. vehicle PBS. (D) Following the same protocol as (B), glycemia, insulin and GLP-1 levels were measured in vehicle-treated mice before and 5 min after glucose gavage. n=14-16/group. p<0.05 vs. baseline within same treatment, #p<0.05 vs. Vehicle PBS at same time point. Data are means±SEM. (E) GLP-1R reporter assay in HEK293 cells treated with control, 5-PAHSA, 9-PAHSA, hydroxystearic acid, palmitate, or GLP-1. n=3wells/condition. *p<0.05 vs. all other groups. Statistical significance was evaluated by unpaired two-tailed Student's t-test or two-way ANOVA with Tukey post-hoc tests. Data are means±SEM.

Figure S4. Related to Figure 4.

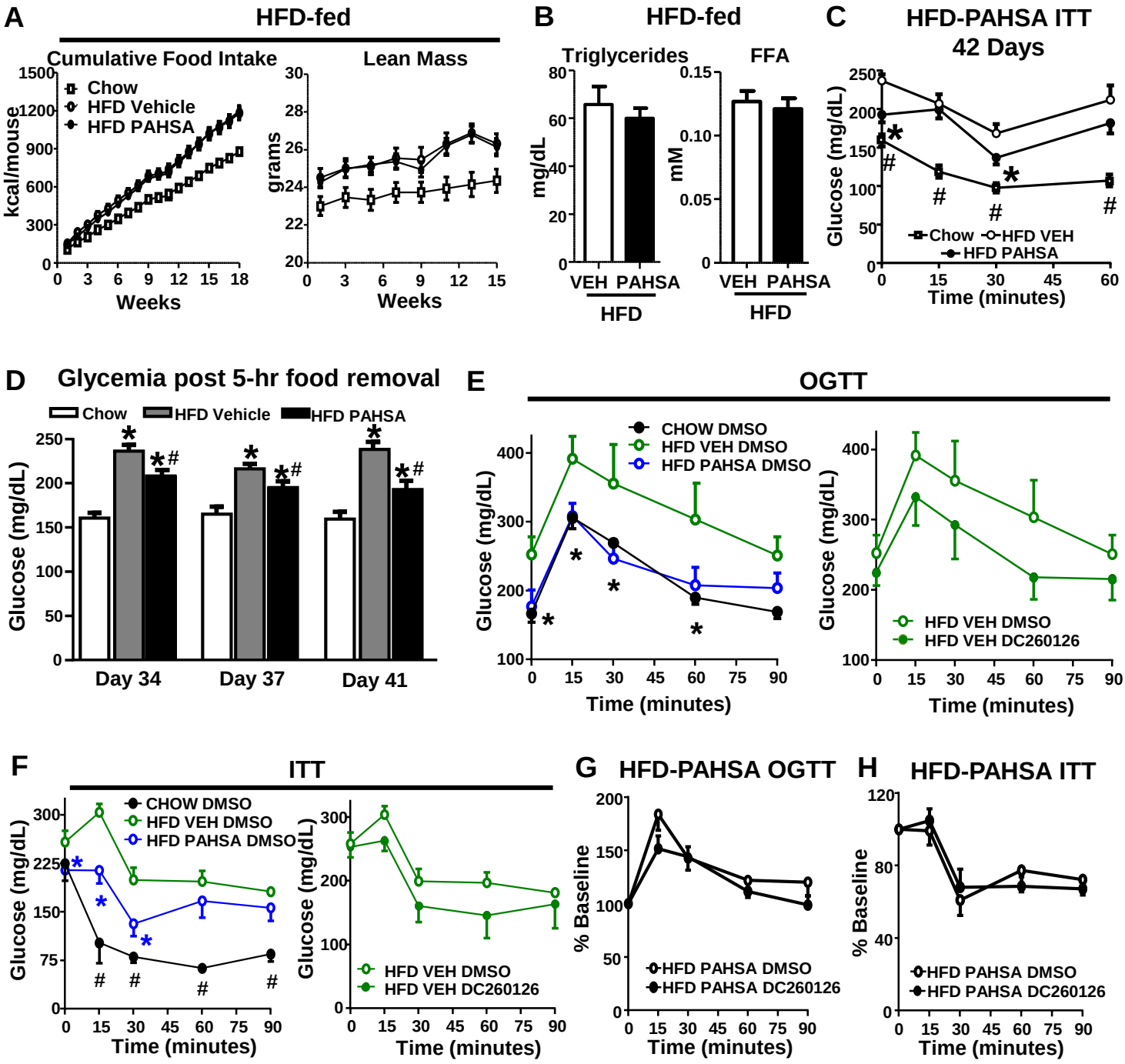

Figure S4. Chronic PAHSA treatment in HFD-fed mice does not affect food intake, lean mass, serum triglycerides or free fatty acids, and improves glycemia and insulin sensitivity. Related to Figure 4.

(A) Cumulative food intake and lean mass in C57bl6 male chow- and HFD-fed mice treated with vehicle or 9-PAHSA via minipumps. n=16/group. (B) Serum triglycerides and free fatty acids (FFA) in vehicle- and PAHSA-treated HFD mice were measured after 4.5 months of treatment. Data are means±SEM. (C) ITT (day 42 of treatment) in vehicle and PAHSA-treated mice. n=8-14/group. *p<0.05 vs. HFD-Vehicle mice; # p<0.05 vs HFD-vehicle and HFD-PAHSA mice. (D) Glycemia 5-hours after food removal in vehicle and PAHSA-treated mice (days 34, 37 and 41 of treatment). n=8-14/group. *p<0.05 vs. Chow-fed mice; # p<0.05 vs HFD vehicle. 5-hours after food removal, mice were injected with either DMSO or DC260126 i.p. and OGTT (E) or ITT (F) was performed 30 minutes later. n=5-6/group. *p<0.05 vs. HFD vehicle DMSO and chow DMSO; # p<0.05 vs. HFD-vehicle-DMSO and HFD-PAHSA-DMSO. Data are means±SEM. 5-hours after food removal, PAHSA-treated mice were injected with either DMSO or DC260126 i.p. and OGTT (G) or ITT (H) was performed 30 minutes later. n=5-6/group. Statistical significance was evaluated by unpaired two-tailed Student's t-test or two-way ANOVA with Tukey post-hoc tests. Data are means±SEM.